High-Speed Floating Potential Measurement with Phase-Flat Response up to 1 MHz for Sub-Ion Scale Turbulence in PANTA

Yuichi KAWACHI[1)]*, Takashi NISHIZAWA[2,3)], Yoshihiko NAGASHIMA[2,3)], Makoto SASAKI[4)], Kenichiro TERASAKA[5)], Yusuke KOSUGA[2,3)], Shigeru INAGAKI[6)], Takuma YAMADA[7)], Naohiro KASUYA[2,3)], Chanho MOON[2,3)], Akihide FUJISAWA[2,3)]

[1)] *Graduate School of Engineering, Nagoya University, Furo-cho, Chikusa-ku, Nagoya 464-8603, Japan*
[2)] *Research Institute for Applied Mechanics, Kyushu University, Fukuoka 816-8580, Japan*
[3)] *Research Center for Plasma Turbulence, Kyushu University, Fukuoka 816-8580, Japan*
[4)] *College of Industrial Technology, Nihon University, Narashino 275-8575, Japan*
[5)] *Department of Computer and Information Sciences, Sojo University, Kumamoto 860-0082, Japan*
[6)] *Institute of Advanced Energy, Kyoto University, Uji 611-0011, Japan*
[7)] *Faculty of Arts and Science, Kyushu University, Motooka, Fukuoka 819-0395, Japan*

(Received 9 December 2025 / Accepted 25 January 2026)

A high-speed floating potential measurement system has been developed for investigating turbulence at frequencies above the ion cyclotron frequency in the PANTA linear plasma device. The system is designed to have a phase-flat response up to 1 MHz, enabling accurate measurement of the phase relationship between floating potential and density fluctuations extending into the high-frequency regime. Initial results show that the attenuation of gain in the high-frequency range is significantly reduced compared to conventional measurements. A cross-phase analysis between the estimated electric field and density fluctuations shows a clear difference.

Keywords: sub-ion scale turbulence, floating potential measurement, turbulent transport

DOI: 10.1585/pfr.21.1302021

Understanding turbulent transport in fusion plasmas remains a critical challenge. Traditional studies have primarily focused on turbulent fluctuations with frequencies below the ion cyclotron frequency (f_{ci}). Recently, however, turbulent fluctuations above f_{ci}, often referred to as sub-ion scale turbulence or nongyrokinetic turbulence, have drawn considerable attention due to their potential role in anomalous transport [1–3]. In our prior work, we have pioneered investigations of these high-frequency fluctuations using ion saturation current measurements with electrostatic probes [4–6].

While ion saturation current I_{is} provides valuable information on density fluctuations, a deeper understanding of turbulent transport requires potential fluctuations measurements. This is because the relative phase and amplitude between density and potential fluctuations are essential for evaluating transport and identifying instabilities. Floating potential V_f measurements are the most commonly employed. However, these are inherently challenging at high frequencies because the sheath resistance between the plasma and the electrode is much higher than in I_{is} measurements [7, 8]. As a result, stray capacitances arising from coaxial cables, connections, and other sources form a low-pass filter, causing signal attenuation and phase delay [9]. This limitation hampers accurate measurements of high-frequency potential fluctuations and their phase relationships with density fluctuations.

In conventional drift-wave turbulence studies, which target fluctuations up to $\sim$ 10 kHz, this effect can often be neglected [10, 11]. In contrast, sub-ion scale turbulence extends over tens to hundreds of kHz, making such stray effects significant. To overcome this limitation, we developed a high-speed measurement system in which an operational amplifier is placed inside the vacuum to perform impedance conversion. The circuit was designed to maintain phase-flat characteristics up to 1 MHz and to avoid oscillations. We validated the circuit through frequency-response measurements using an emulated sheath resistance load and compared experimental data acquired with the new system to those obtained using conventional circuits.

Floating potential V_f is defined as the potential at which electron and ion currents balance, and thus no net current flows into the measurement circuit. A high input impedance is therefore required to obtain the true V_f . In practice, large resistors and voltage dividers are used, and signals are transmitted through coaxial cables to suppress noise and crosstalk. However, the stray capacitance of the coaxial cables, together with the high impedance resistance, forms a low-pass filter that attenuates high-frequency components and introduces phase delay. Such effects can be mitigated by either eliminating the

*Corresponding author's e-mail: y-kawachi@energy.nagoya-u.ac.jp

cable connection immediately after the high-impedance section or adding a compensation capacitor.

In practical plasma measurements, however, the plasma sheath resistance R_{sheath} between the plasma and the electrode must also be considered. This finite R_{sheath} , combined with the cable capacitance, forms a low-pass filter as discussed above. Consequently, high-frequency components of V_f are attenuated, accompanied by significant phase delay. The R_{sheath} can be roughly estimated as $R_{sheath} = T_e/I_{is}$, where T_e is the electron temperature. Under the experimental conditions of this study, I_{is} is a few milliamperes and the electron temperature is approximately 1–2 eV, giving an estimated R_{sheath} of a few hundred ohms to below 1 kΩ. For example, with a 5 m coaxial cable (100 pF/m), the sheath resistance R_{sheath} = 1 kΩ and the resulting 500 pF stray capacitance form a low-pass filter with a cutoff frequency of about 318 kHz. The gain decreases by −3 dB at 318 kHz, and the phase delay at this frequency reaches $-\pi/4$ rad. In general, avoiding phase delay requires a cutoff frequency several times higher than the targeted measurement frequency band. Accurate measurement of phase differences between density and potential fluctuations above several tens of kHz therefore requires mitigation of this low-pass effect.

Three approaches exist for high-speed floating-potential measurements: capacitive probes, capacitance neutralization, and impedance transformation. In capacitive probes, an insulating layer is introduced between the plasma and the electrode, enabling capacitive rather than resistive coupling [7, 12]. This technique is effective when only high-frequency components are of interest, as low-frequency components are attenuated. Capacitance neutralization and impedance transformation both use operational amplifiers to compensate the sheath impedance, effectively transforming the sheath impedance into the lower output impedance of the amplifier [13, 14]. In addition, capacitance neutralization drives the capacitance of the coaxial cable, actively cancelling the cable capacitance, a method also referred to as a “driven shield” or “active guard” [12, 15].

Both techniques allow high-frequency measurements without attenuation; however, driving the capacitive load of the coaxial cable with an operational amplifier can cause instability due to its phase characteristics. Capacitance neutralization is particularly prone to oscillation [15, 16]. In this study, impedance transformation was adopted to ensure stable operation, enabling the development of a high-speed and robust floating-potential measurement system.

The circuit developed in this study is shown in Fig. 1(a-3). In this design, a voltage divider and an operational amplifier are placed immediately behind the probe electrode to transform the sheath resistance. Because the sheath resistance fluctuates, a 1 MΩ resistor, sufficiently larger than the sheath resistance (≤1 kΩ), was used to ensure accurate measurement. To achieve a flat gain and phase response across a wide bandwidth and to provide sufficiently high input impedance, the FET-input operational amplifier AD8066, with a bandwidth of 145 MHz, was selected. To suppress oscillations due to insufficient phase margin, the operational amplifier was operated not as a unity-gain buffer, which is intrinsically susceptible to oscillation, but as a non-inverting amplifier with a gain of 5. An additional 50 Ω output resistor was included for both oscillation suppression and impedance matching. The circuit was implemented on a compact printed circuit board mounted inside the probe shaft, as shown in Fig. 1(b).

To evaluate the frequency response of the circuit, a 1 kΩ

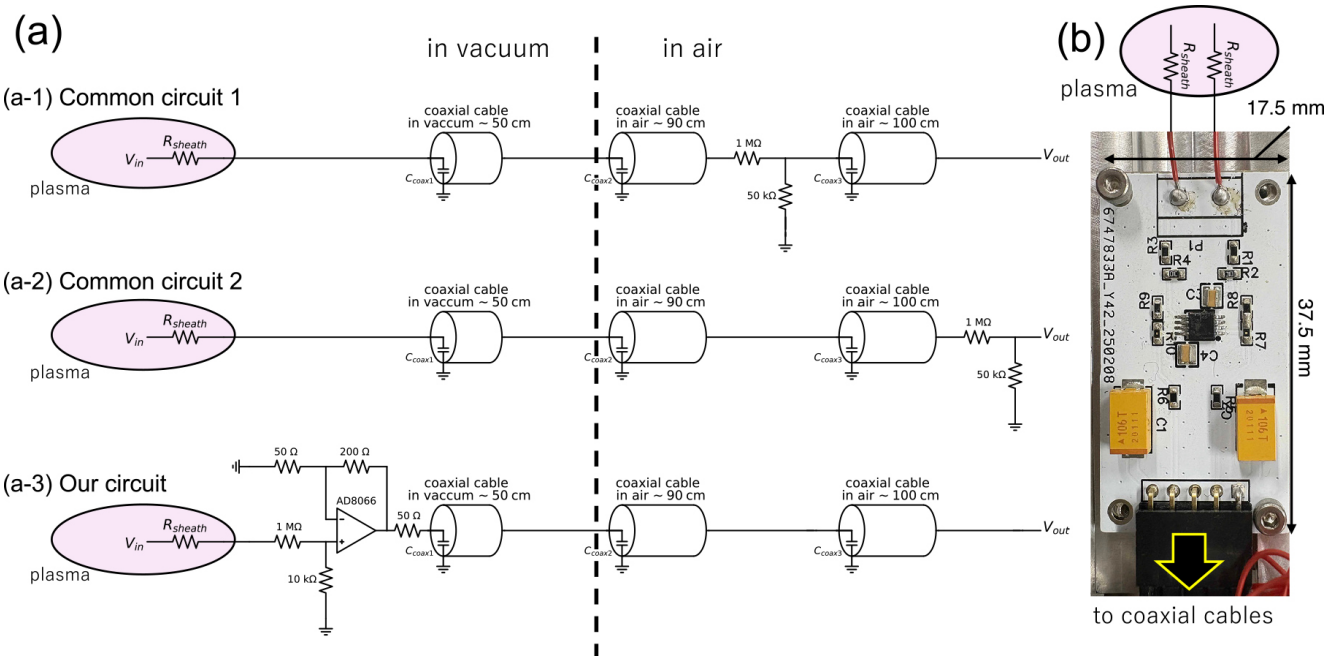

Fig. 1. (a) Schematic diagrams of three V_f measurement circuits for comparison. All coaxial cables have cable (stray) capacitance. (b) A photograph of the circuit installed in vacuum for high-speed V_f measurement.

resistor was used to emulate the sheath resistance R_{sheath}, and the frequency characteristics were measured. For comparison, two commonly used circuit configurations—both lacking explicit consideration of R_{sheath}—were also evaluated, shown in as Figs. 1(a-1) and (a-2). The two differ in whether the coaxial cable is placed before or after the voltage divider. This comparison illustrates the influence of the low-pass filtering caused by the voltage divider and cable capacitance when no compensation is applied. The total coaxial cable length was kept constant at 2.4 m (stray capacitance ~ 240 pF) for all three circuits.

Figure 2 shows the Bode plots for the three circuits. In the common circuits, gain starts to drop at 50–100 kHz, with phase delay appearing at even lower frequencies, reaching about $\pi/4$ at 100 kHz. Placing the cable after the voltage divider without compensation further degrades the response. These results demonstrate that conventional floating-potential circuits distort signals above several tens of kilohertz due to phase delay, making them unsuitable for turbulence-driven transport measurements that rely on the phase relation between density and potential. In contrast, the circuit developed in this study has a much wider bandwidth, with the gain roll-off starting only near 10 MHz and the phase remaining nearly flat up to 1 MHz. This stable gain response prevents degradation of the signal-to-noise ratio, and the flat phase response avoids phase-delay–induced errors in transport evaluations, thereby allowing accurate phase measurements even for turbulence with frequency components of several hundred kilohertz or more.

The developed high-speed V_f measurement system was tested in the PANTA linear plasma devic [11]. The PANTA device has a cylindrical vacuum chamber with a diameter of 0.45 m and a length of 4 m, equipped with a set of solenoidal coils that generate an axial magnetic field of 0.0235 T. The plasma is produced by RF of 7 kW and 7 MHz. Typical electron density n_e and electron temperature T_e are $n_e \sim 10^{18}$ m^{-3} and $T_e \sim$ 1–2 eV, respectively. Under these conditions, the broadband high frequency fluctuations above the ion cyclotron frequency ($f_{ci} \sim$ 8.9 kHz) have been observed in previous studies [4–6].

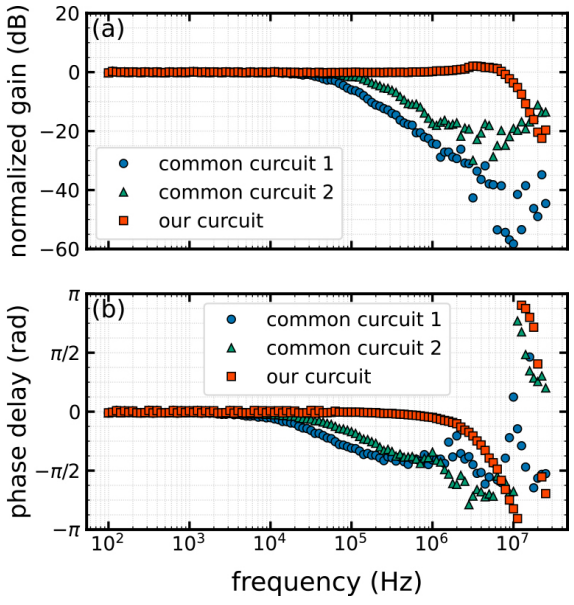

Fig. 2. Bode plots of three V_f measurement circuits.

The high-speed V_f measurement system was connected to SUS304 probe tips and to an isolation digitizer via a ~ 0.5 m coaxial cable in vacuum and a ~ 0.9 m coaxial cable in air. The V_f signals were acquired at a sampling rate of 2 MHz by the isolation digitizer, and a 400 kHz internal low-pass filter was applied to avoid aliasing. The probe system was installed 1.375 m downstream from the RF antenna, and the radial position was set to r = 40 mm. For reference, the conventional 64-channel probe array system was also operated at a position 1.885 m from the RF antenna and at the same radius of 40 mm [10]. Each probe tip in the conventional system was connected to the circuit box through approximately 1.5 m of coaxial cable in vacuum and another 1.5 m in air. A voltage divider was placed after this coaxial cable. Following the voltage divider, the signals were transmitted through an additional 3 m of coaxial cable to another isolation digitizer, with compensation applied for the capacitance of this 3 m cable. The conventional system acquired data at a sampling rate of 1 MHz with a bandwidth of 200 kHz.

Measured V_f signals using the high-speed system are shown in Fig. 3(a). The power spectrum density are shown in Fig. 3(b). For comparison, the V_f signals obtained using the conventional system are also shown. Although a direct comparison is complicated by differences in digitizer bandwidth and measurement locations, it is evident that the high-speed system preserves high-frequency components around 100 kHz better than the conventional system.

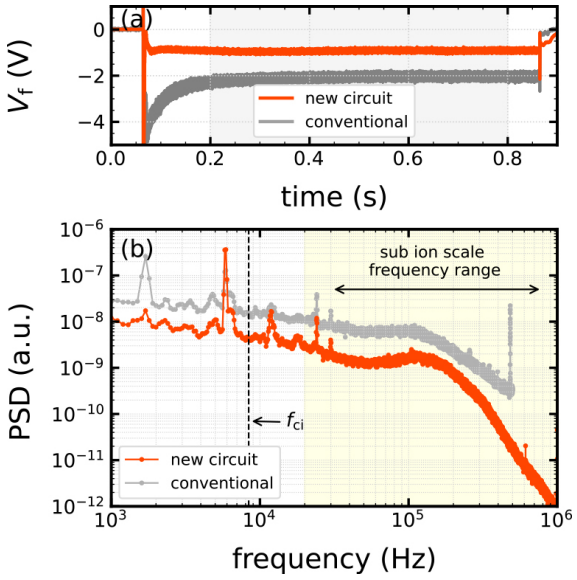

Fig. 3. (a) Typical temporal evolution and (b) power spectral density measured. The yellow shaded area indicates the frequency range of sub-ion-scale turbulence. Red and gray lines indicate the results obtained by the high-speed system and the conventional system, respectively.

To evaluate turbulence-driven transport and identify underlying instabilities, the relative phase and amplitude between density and potential fluctuations are essential. When the drift approximation holds, azimuthal electric field E_y fluctuations generate radial $E \times B$ flows, and transport is driven when a finite phase shift exists between density and electric field fluctuations. Therefore, the phase difference was analyzed and compared between the high-speed V_f measurement system and the conventional system.

For the high-speed V_f measurement system, three probe tips with 2 mm spacing were used: the central pin measured I_{is}, while the two outer pins measured V_f. The E_y component was estimated from the potential difference between the outer pins. Both I_{is} and the high-speed V_f signals were acquired using the same broadband digitizer. For the conventional system, a similar set of three probe tips with 3.9 mm spacing was used.

Cross-spectral analysis was performed between the I_{is} and the estimated E_y, and the resulting coherence and phase differences are shown in Figs. 4(a) and (b). At low frequencies (a few kilohertz), the phase differences obtained from the two circuits agree reasonably well. We note that the remaining discrepancies in this range may be attributed to the low coherence. For example, around 10–20 kHz, the phases differ where the coherence is low—except near specific peaks—whereas near the peaks with high coherence, the phases show good agreement. At higher frequencies, corresponding to the sub-ion-scale turbulence range, the conventional circuit exhibits a markedly different phase response due to its significant phase delay. In contrast, the new circuit maintains a nearly constant phase difference up to about 200 kHz, whereas the conventional circuit shows a phase shift exceeding π rad relative to the new circuit. This result demonstrates that the new high-speed floating-potential circuit has a strong capability for accurate phase-difference measurements.

We note that both cicurits show a drop of coherence at higher frequencies. This is due to the turbulence wavelength becoming comparable to the probe spacing, which can cause the measured potential to cancel out, effectively reducing the E_y to zero. Concequently, the potential difference between the two probe tips can no longer be regarded as a proper measure of the local electric field in the 0.3–1 MHz range. This limitation can be overcome by reducing the probe spacing in future experiments.

Such accurate phase measurements are also crucial for investigating nonlinear interactions using cross-frequency methods, including biphase analysis. In the present experiment, however, the applicable frequency range for such analyses is limited by the digitizer bandwidth rather than by the measurement circuit. The use of higher-bandwidth digitizers would allow the full capability of the high-speed floating potential measurement system to be exploited for cross-frequency analyses.

In summary, a high-speed floating potential measurement system with a phase-flat response up to 1 MHz has been developed for investigating high-frequency turbulence in the PANTA linear plasma device. The system employs an impedance transformation circuit using an operational amplifier placed inside the vacuum chamber, effectively mitigating the low-pass filtering effects caused by sheath resistance and cable capacitance. Frequency response measurements confirmed the circuit's wide bandwidth and minimal phase delay. Initial plasma measurements demonstrated that the new system preserves high-frequency components and enables accurate phase measurements between density and electric field fluctuations, essential for understanding turbulence-driven transport mechanisms.

This work was supported in part by JSPS KAKENHI under Grant Nos. JP25K00986, JP24K06996, JP23K13082, JP21H01066, the Collaborative Research Program of Research Institute for Applied Mechanics Kyushu University, the grant of OML Project by the National Institutes of Natural Sciences (NINS program No, OML012511), and Nitto Foundation. The authors would like to thank Mr. J. Nagaya and Mr. I. Niiya, for their support in the experiment.

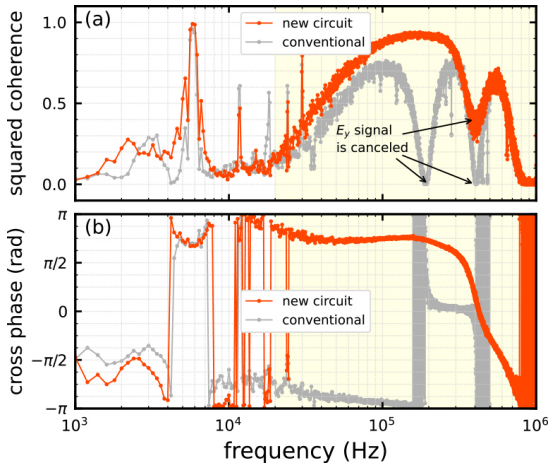

Fig. 4. (a) Squared coherence and (b) cross-phase between I_{is} and the estimated azimuthal electric field fluctuations measured by the high-speed V_f measurement system (red) and the conventional system (gray).

[1] R.O. Dendy *et al.*, Phys. Rev. Lett. **130**, 105102 (2023).
[2] M. Raeth and K. Hallatschek, Phys. Rev. Lett. **133**, 195101 (2024).
[3] V.V. Mikhailenko *et al.*, Phys. Rev. Lett. **31**, 032307 (2024).
[4] Y. Kawachi *et al.*, Sci. Rep. **12**, 19799 (2022).
[5] Y. Kawachi *et al.*, Plasma Phys. Control. Fusion **65**, 115001 (2023).
[6] Y. Kawachi *et al.*, Phys. Plasmas **31**, 044502 (2024).
[7] J.A. Schmidt, Rev. Sci. Instrum. **39**, 1297 (1968).
[8] F.F. Chen, *In Proceedings of the IEEE-ICOPS Meeting*, (Jeju, Korea, 5 June 2003).
[9] Y. Nagashima *et al.*, Rev. Sci. Instrum. **96**, 093509 (2025).
[10] T. Yamada *et al.*, Nat. Phys. **4**, 721 (2008).
[11] S. Inagaki *et al.*, Sci. Rep. **6**, 22189 (2016).
[12] T. Nishizawa *et al.*, Rev. Sci. Instrum. **89**, 10J118 (2018).
[13] Y. Tanaka *et al.*, Plasma Fusion Res. **2**, S1090 (2007).
[14] K. Terasaka *et al.*, Rev. Sci. Instrum. **85**, 113503 (2014).
[15] A. Rich, *Analog Devices Application Note AN-347*, (1983).
[16] E. Spinelli and F. Reverter, IEEE Trans. Instrum. Meas. **59**, 458 (2010).